Transcriptional control of a rRNA promoter of the nodulating symbiont *Sinorhizobium meliloti*

Michelle Rosado, Daniel J. Gage *

University of Connecticut, Department of Molecular and Cell Biology, 91 N. Eagleville Rd., U-44, Storrs, CT 06269, USA

Abstract

We constructed a stable, low-copy-number plasmid containing a fusion between a *Sinorhizobium meliloti* rRNA promoter and *gfp(mut3)*. When transformed into *S. meliloti* the resulting strain, Rm1021/pKW1, fluoresced in proportion to its growth rate during balanced growth. This strain also showed an unexpected behavior when grown to stationary phase in TY medium: the average cellular fluorescence increased through mid-exponential phase then decreased dramatically. The explanation for this appears to be that transcription from the rRNA promoter was shut off in mid-exponential phase and intracellular Gfp was diluted by continued cell growth. © 2003 Federation of European Microbiological Societies. Published by Elsevier B.V. All rights reserved.

Keywords: *Sinorhizobium meliloti*; Guanosine tetraphosphate; rRNA; Ribosome

1. Introduction

Sinorhizobium meliloti, a member of the α-Proteobacteria, is found free-living in soil but can also live as intracellular symbionts of alfalfa and several other plants belonging to the family Leguminosae [1–6]. The symbiotic form resides in root nodules and is able to reduce atmospheric nitrogen to ammonia, thus providing its host plant with the ability to populate environments which are marginal due to low levels of available nitrogen.

S. meliloti is very flexible metabolically because it carries a large number of genes for the import and catabolism of exogenous growth substrates. Genome sequencing revealed that 12% of its 6200 genes are dedicated to transport. Most of these are dedicated to the import of amino acids, peptides, and carbohydrates [7,8]. Such a large repertoire of genes encoding import functions indicates that *S. meliloti* can probably utilize a large number of carbon sources found in soil and near plant roots. Laboratory investigations have confirmed the genomic data, and have shown that this species can utilize a wide variety of substances as growth substrates that support a wide range of growth rates [9,10].

In some species of bacteria, high rates of growth are supported mainly by high numbers of ribosomes, rather than by especially high rates of ribosomal transit along mRNAs. In media that allow fast growth, *Escherichia coli* has relatively many ribosomes that move at a characteristic rate along mRNA. In media that support a slower growth rate, *E. coli* has fewer ribosomes which move at a characteristic rate that is only somewhat slower than the rate seen in faster growing cells [11–13]. While rates of DNA replication, transcription, cell wall synthesis, and other cellular activities must respond efficiently and robustly to changes in growth rate, it is thought that control of ribosome synthesis in response to changes in growth rate is important because ribosomes are large, complex, assemblages that are expensive to synthesize. In *E. coli* ribosome levels are controlled mainly by the rate of production of rRNA, which is controlled mainly by the rate at which rRNA transcription is initiated from the upstream-most rRNA promoter, termed the P1 promoter [14]. In *E. coli* ribosome levels are proportional to growth rate, and the rate of transcription from the *rrn* P1 promoters is proportional to the square of the growth rate [14]. It has been estimated that under conditions of rapid growth half of all transcription in *E. coli* is dedicated to the production of ribosomal RNA [15]. Because of the

---

* Corresponding author. Tel.: +1 (860)-486-3092;
Fax: +1 (860)-486-1784.

E-mail address: gage@uconnvm.uconn.edu (D.J. Gage).

relationship between rRNA transcription and growth rate reporter genes such as *lacZ*, *luxAB* and *gfp* fused to rRNA promoters can be used to monitor transcriptional activity of rRNA promoters, and indirectly, bacterial growth rate [11,16–19].

We have fused a fast-folding variant of Gfp to a *S. meliloti* rRNA promoter and used the fusion to monitor transcription from that promoter. Work described below shows transcription from the promoter increases with increasing steady-state growth rate. The promoter also shows an unusual pattern of expression during growth from lag to stationary phase in complex medium.

2. Materials and methods

2.1. Bacterial strains, growth media and chemicals

Strains and plasmids are listed in Table 1. Bacteria were grown in tryptone-yeast medium (TY medium: 6 g tryptone, 3 g yeast extract, 0.38 g $CaCl_2$ per liter), TY+0.4% glucose, or in M9 salts [20] containing glycerol, succinate or fumarate at 0.4% (w/v). Streptomycin was used at 500 μg ml^{-1}, chloramphenicol at 200 μg ml^{-1} and tetracycline at 2.5 μg ml^{-1}. AlexaFluor 488 standards were purchased from Molecular Probes (Eugene, OR, USA) as was the InSpeck Green Calibration kit.

2.2. Plasmid construction

The promoter region of *rrnB* was amplified from Rm1021 genomic DNA using primers rRNA-up (5′-CTA-TTGGCTGATCTGCCACC-3′) and rRNA-down (5′-CC-AGCGTTCGTTCTGAGCCA-3′). *Bam*HI linkers were ligated to the 751-bp amplification product and it was cloned into *Bam*HI-cut pBluescript SK(−), giving pDG76. The amplification product was removed as a *Bam*HI fragment from pDG76 and cloned into *Bam*HI-cut pDG65, a pVO155-based plasmid that contained *gfp(mut3)* under the control of a constitutive *trp* promoter fragment from *Salmonella typhimurium* [21–23]. This replaced the *trp* promoter fragment with the *rrnB* promoter fragment, and resulted in the *gfp(mut3)* gene being flanked upstream by the *rrnB* promoter, and downstream by a *trp* transcriptional terminator. The resulting plasmid was pDG78. Next, the terminator-rRNA promoter-*gfp(mut3)* cassette was removed by digesting pDG78 with *Pst*I and *Kpn*I. The cassette was cloned into the high-copy-number, broad-host-range plasmid pMB393, giving pDG79. We were unable to move this plasmid into *S. meliloti*, perhaps because cells could not tolerate high numbers of plasmid-borne rRNA promoters. The terminator-rRNA promoter-*gfp(mut3)* cassette was removed from pDG79 as an *Xba*I-*Kpn*I fragment and cloned into the stable, low-copy-number, broad-host-range plasmid pHC41, giving plasmid pKW1 (Fig. 1) The rRNA promoter region of pKW1 was checked by sequencing. A promoter-deletion control was constructed by dropping a 515-bp *Sal*I fragment from pKW1. This removed the rRNA P1 region and upstream sequences. The resulting plasmid was pTSM2 (Fig. 1).

2.3. Balanced growth experiments

Strains Rm1021/pKW1 and Rm1021/pTSM2 were grown to stationary phase in 2.5 ml of medium in 18×150-mm tubes at 30°C. They were then diluted 1:100 in 25 ml of prewarmed medium in 250-ml flasks and shaken at 250 rpm at 30°C. When the OD_{415} reached 0.08–0.10 the culture was diluted 1 to 20 into 25 ml of prewarmed medium. Multiple samples were collected after the second dilution, before the cultures went above an OD_{415} of 0.1. Optical density was measured by reading 100 μl of culture in a 96-well microtiter dish with a Bio-Rad 550 plate reader. Because of the short path length the optical density is about three times less than what would have been observed using a cuvette with a standard 1-cm

Table 1
Strains and plasmids

	Relevant characteristics	Source
Strains		
Rm1021	Wild-type (Sm^r)	[38]
XL1 Blue MRF′ Kan	Cloning strain (Kan^r)	Stratagene
Plasmids		
pDG65	Contains a *trp* terminator in front of *gfp(mut3)*	This study
pDG71	Constitutively expressed *gfp(mut3)* gene cloned into the stable, low-copy-number, broad-host-range plasmid pHC41	[39]
pDG76	pBluescript containing a PCR-amplified copy of the *S. meliloti rrnB* promoter	This study
pDG78	pDG76 with the *S. meliloti rrnB* promoter inserted between the *trp* terminator and *gfp(mut3)*	This study
PDG79	pMB393 containing the terminator-p*rrnB*-*gfp(mut3)* cassette from pDG78	This study
pKW1	pHC41 containing the terminator-p*rrnB*-*gfp(mut3)* cassette from pDG79	This study
pTSM2	pKW1 with a 515-bp *Sal*I fragment removed from the *rrnB* promoter	This study
pHC41	Stable, low-copy-number, broad-host-range plasmid	[28]
pMB393	High-copy-number, broad-host-range plasmid	[40]
pBluescript SK(−)	Cloning vector	Stratagene
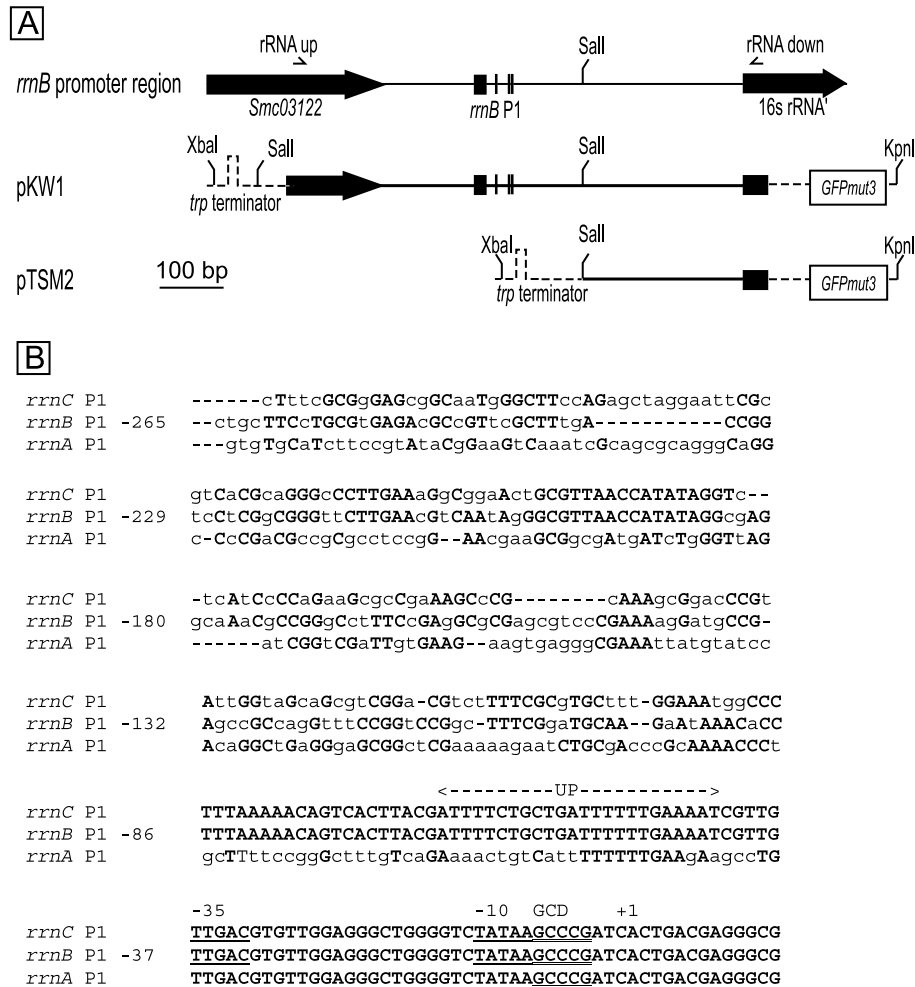
Fig. 1. Promoter regions of the three rRNA operons in *S. meliloti*. A: Top shows a schematic diagram of the *rrnB* promoter region of *S. meliloti*. Below are maps showing regions cloned into plasmids pKW1 and pTSM2. Solid black lines and boxes represent cloned *S. meliloti* DNA, dashed lines and white boxes represent plasmid vector DNA. B: Aligned sequence of the three *S. meliloti* rRNA P1 promoter regions. Bases present at the same location in two or more sequences are shown in bold typeface. Also highlighted are the presumptive −10, −35, +1 and UP sequences, as well as the putative GC-rich discriminators (GCD). The location of the +1 site is from Gustafson et al. [18].

path length. Samples for culture fluorescence, single-cell fluorescence and RNA levels were taken at various times and cell pellets were frozen in 120 μl of 15% glycerol at −80°C until all samples were collected.

2.4. One-step growth experiments

Strains Rm1021/pKW1 and Rm1021/pTSM2 were grown to stationary phase in 2.5 ml of TY medium containing 500 μg ml^{-1} streptomycin and 2.5 μg ml^{-1} tetracycline in 18×150-mm tubes at 30°C. They were then diluted into 100 ml of prewarmed TY medium with 2.5 μg ml^{-1} tetracycline in 1000-ml flasks such that the OD$_{415}$ was about 0.005. They were shaken at 250 rpm at 30°C. Samples for culture fluorescence, single-cell fluorescence and stable RNA levels were taken at various times and cell pellets frozen in 120 μl of 15% glycerol at −80°C until all samples were collected.

2.5. Culture fluorescence determination

Culture samples were thawed on ice and fluorescence of the cells was measured using a CytoFluor 4000 fluorimeter with excitation at 485 nm and emission at 508 nm. Fluorescence was corrected for cell number by dividing sample fluorescence by its optical density at 415 nm. Optical density at 415 nm was determined using a Bio-Rad 550 plate reader. In order to remove variability due to fluorimeter warm-up times, or bulb intensity, the relative bacterial fluorescence was standardized using an AlexaFluor 488 reference curve. The fluorescence of 0–3.5 μM AlexaFluor 488 was determined at the same time as was bacterial fluorescence, and bacterial fluorescence was expressed in those units. For example, 100 μl of bacteria with a fluorescence of 0.1 μM were as bright as 100 μl of 0.1 μM AlexaFluor 488 read under the same conditions.

2.6. Single-cell fluorescence determination

Samples for single-cell analysis were mounted on poly-lysine-coated slides and epifluorescent images were taken with a Qimaging Retiga EX chilled CCD camera using a $60 \times$, 0.7 NA, objective on a Nikon Eclipse 300 microscope. Bacterial fluorescence was corrected by subtracting the background fluorescence from each image. For each sample, the average pixel intensity of 50–200 bacteria was determined, and corrected for autofluorescence of the control strain Rm1021/pTSM2. In order to reduce variability caused by sample mounting, microscope settings, and mercury bulb age and positioning, bacterial fluorescence was standardized using reference beads. The fluorescent beads were imaged at the beginning of each microscope session, and quantitated with the same methods used for quantitative imaging of bacteria. The fluorescence of bacterial cells in these experiments was similar to the fluorescence of 0.3% standard beads in the InSpeck Calibration kit from Molecular Probes (Eugene, OR, USA). Thus, bacterial fluorescence was reported in the same units as these beads (%). Bacterial fluorescence was imaged using a filter set with a 465–495-nm excitation filter and a 515–555-nm emission filter. Image quantification was done with NIH Image.

2.7. Stable RNA levels

Culture pellets were precipitated on ice for 30 min with 50 µl of 10% trichloroacetic acid (TCA). The precipitate was spun down and washed with 100 µl of 10% TCA, and resuspended in 200 µl 5% TCA. This was incubated at 95°C to hydrolyze nucleic acids. The hydrolysate was spun down and 150 µl of supernatant was combined with 150 µl of orcinol reagent [24], incubated at 100°C for 20 min, and then cooled on ice. A 200 µl was read in a Bio-Rad 550 microtiter plate reader using a 655-nm filter. Yeast tRNA was used as a standard.

2.8. Measurement of transcript levels by reverse transcription polymerase chain reaction (RT-PCR)

RNA was purified from cell pellets, and 1 µg of each RNA sample was spiked with 10^9 copies of a control RNA encoding a kanamycin resistance protein (Promega). The samples were then reverse-transcribed at 42°C for 1 h using ImProm-II reverse transcriptase (Promega). Primers used were 5′-ATCCAGCAGCTGTTACAAACTCA-3′ for *gfp* and oligo d(T$_{15}$) for the kanamycin control. Following reverse transcription, 0.01 µl of the 50 µl reaction was amplified by PCR using primers *gfp*-up (5′-ACCAT-GTGGTCTCTCTTTTCGTTG-3′) and *gfp*-down (5′-AT-CCCAGCAGCTGTTACAAACTCA-3′). This generated a 687-bp amplification product from *gfp* cDNA. Separately, 0.01 µl of each 50 µl reverse transcription reaction was also amplified with primers specific for the kanamycin

control cDNA (5′-GCCATTCTCACCGGATTCAGT-CGT-3′ and 5′-AGCCGCCGTCCCGTCAAGTCA-3′) which generated a 323-bp product. 50 µl PCR reactions were cycled as follows: 2 min at 94°C for initial denaturation, then 1 min at 94°C, 1 min at 58°C, 2 min at 72°C for 34 cycles, followed by a final extension at 72°C for 5 min. Using this protocol the PCR product formed was proportional to the amount of input cDNA for *gfp* and control cDNAs. All samples were also amplified following a mock reverse transcription step to ensure that there was no DNA contamination present that could give rise to PCR products.

3. Results and discussion

3.1. Sequence analysis of three S. meliloti rRNA promoter regions, and construction of a prrnB-gfp reporter

S. meliloti contains three rRNA operons on its 3.65-Mb chromosome. These operons are similar in overall structure to most other bacterial rRNA operons. Each encodes a 16S, 23S and 5S rRNA along with tRNAs that decode alanine and methionine codons [8,25]. The operons are identical in sequence from their promoter regions through the met-tRNA genes that are at their ends. The rRNA operons begin near base numbers 81 150, 2 812 000 and 3 214 400 on the chromosome [8,25,26] and are referred to as *rrnC*, *rrnA* and *rrnB* respectively in this paper, following the nomenclature of Gustafson et al. [18]. The putative P1 −10, −35, GC-rich discriminators, and UP elements of all three promoter regions were easily identified because of their similarity to these regions in other bacterial rRNA promoters (Fig. 1) [19,27]. The GC-rich discriminators, −10, and −35 regions are identical in all three *S. meliloti* rRNA promoters. The UP elements, and upstream DNA differ among the three promoter regions, with those from *rrnC* and *rrnB* being most similar. The DNA upstream of the UP elements contains some regions that are conserved among the three promoters, but it was difficult to discern any sequences that may act as binding sites for regulatory proteins (Fig. 1).

The promoter region of *rrnB* was cloned by high-fidelity PCR. The amplified 751-bp fragment was cloned downstream of a transcriptional terminator and in front of *gfp*(*mut3*) (Fig. 1). The resulting terminator-p*rRNA*-*gfp*(*mut3*) cassette was cloned into the stable, low-copy-number plasmid pHC41 [28] giving plasmid pKW1. A control plasmid, pTSM2, that lacked the *rrnB* promoter was also constructed (Fig. 1).

3.2. Fluorescence of the prrnB-gfp reporter during batch growth in a complex medium

We initially tested the response of the p*rrnB*-*gfp* reporter to varying growth rate by batch culturing strains

Rm1021/pKW1 and Rm1021/pTSM2 in a TY growth medium and determining the fluorescence of cells over the course of growth. Both single-cell fluorescence measurements and fluorescence measurement by fluorimetry showed that cells of Rm1021/pKW1 increased in brightness up through the mid-exponential section of the growth curve (Fig. 2). At that point the cells stopped increasing in brightness and over the remainder of the growth curve the average fluorescence per cell decreased dramatically. By the time the cells reached stationary phase their fluorescence had decreased to background levels. This result was unexpected because transcription rates of rRNA promoters are generally high when rates of cell growth are high.

The above result could possibly have been explained by degradation of Gfp. Even though Gfp is generally very stable [29], it was important that we test its stability in *S. meliloti*. We repeated the experiment and stopped protein synthesis in mid-exponential phase by adding chloramphenicol to the culture. Gfp was not synthesized after
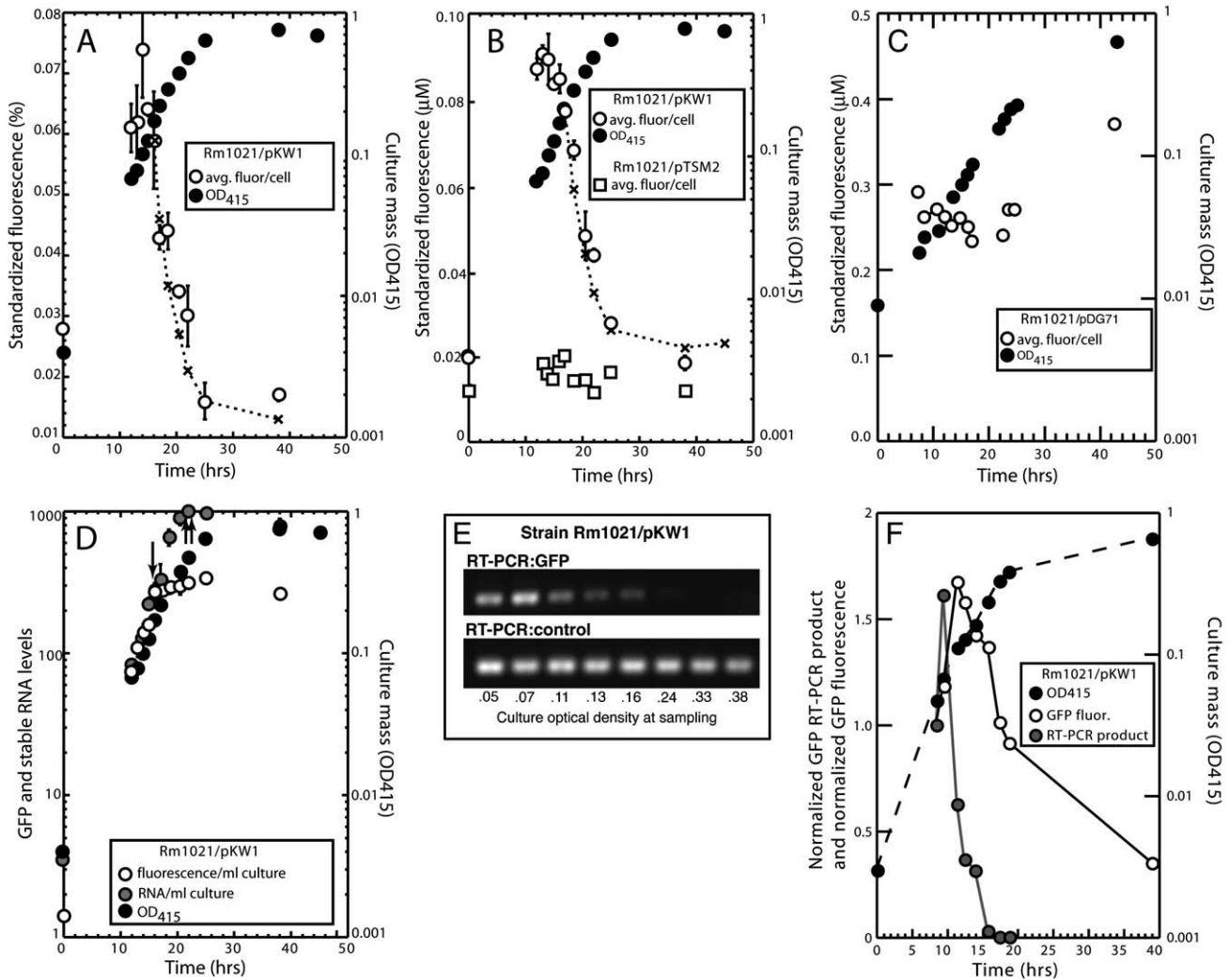
Fig. 2. Behavior of strain Rm1021/pKW1 during growth to stationary phase in TY medium. A: Culture optical density (closed circles) and average fluorescence per cell (open circles) were determined for three parallel cultures. Dashed line shows how the values of Gfp per cell would decline if the p*rrnB* promoter driving *gfp* expression was completely shut off 2 h after peak fluorescence, and the Gfp present in each cell was diluted as the culture continued to grow. Fluorescence values are quantitated in units of InSpeck standard bead brightness. B: Same as in A except fluorescence per cell was determined by fluorimetry. Squares show the average fluorescence per cell of control strain Rm1021/pTSM2. Fluorescence values are quantitated in units of μM AlexaFluor 488. C: Same as B except optical density and fluorimetry results for strain Rm1021/pDG71 are shown. D: Optical density, total RNA and total fluorescence per ml of culture are plotted. The single arrow indicates the time at which fluorescence stopped accumulating in the culture, the double arrow indicates when RNA stopped accumulating in the culture. RNA and fluorescence levels were normalized to a value of 100 at $t = 12$ h. Error bars show S.E.M. in panels A, B and D. E: RT-PCR products from samples obtained during growth of strain Rm1021/pKW1 in TY medium. Top panel shows RT-PCR products from p*rrnB*-driven *gfp* mRNA, bottom panel shows RT-PCR products from a positive control mRNA that was added to each sample before reverse transcription. Numbers at the bottom indicate the optical density of the culture at the various sampling times. F: Optical density (filled black circles), fluorimetry results (open circles), and amounts of p*rrnB*-*gfp* RT-PCR product for the culture used in the RT-PCR experiments shown in E. The *gfp* RT-PCR products were quantitated by densitometry and corrected by dividing the *gfp* RT-PCR product by the control RT-PCR product. The fluorimetry and RT-PCR data were normalized to a value of 1.0 at $t = 9$ h.

chloramphenicol addition, and the half-life of the preexisting Gfp was more than 12 h (data not shown).

The original experiment was repeated using a plasmid that differed from pKW1 only in that the promoter was not the *rrnB* promoter, but a constitutively expressed fragment of the *S. typhimurium trp* promoter [30]. This strain, Rm1021/pDG71, did not show a decline in fluorescence during mid-exponential phase (Fig. 2C). This result, combined with the demonstrated long half-life of Gfp, indicated that the decline seen with strain Rm1021/pKW1 at mid-exponential was not likely due to lack of folding or degradation of Gfp brought on by a change in culture conditions or cell physiology. The declining fluorescence levels after mid-exponential phase were most likely due to a stop, or dramatic decrease, in transcription from the *rrnB* promoter that was driving *gfp* expression. In fact, the decline in fluorescence per cell could be modeled by assuming a complete lack of Gfp synthesis 2–3 h after peak fluorescence, followed by dilution of the existing Gfp by the increase in culture mass that takes place as the cells grow to stationary phase (see dashed line in Fig. 2A,B).

To investigate the possibility that *rrnB-gfp* transcript levels fell during mid-exponential phase, RNA was isolated from culture samples of Rm1021/pKW1 during growth in TY. RT-PCR of *rrnB-gfp* mRNA in these samples showed that levels of transcript from the *rrnB*-driven reporter fell precipitously just before Gfp fluorescence began to decline (Fig. 2E,F). The decline in *rrnB-gfp* transcript levels was much quicker than the decline in Gfp fluorescence, which was expected given the short half-life of most mRNA molecules in bacteria. Ideally, rRNA levels originating from each of the rRNA operons would have been measured separately by RT-PCR, rather than the *gfp* reporter. However, the fact that the rRNA operons are identical from the P1 −35 box to the end of the operon precluded that possibility.

Measurement of stable RNA and total fluorescence of the cultures during batch growth showed that while Gfp stopped accumulating in mid-exponential phase, stable RNA continued to accumulate until cells reached stationary phase (Fig. 2C). This suggests that transcription from the *rrnA* or *rrnC* must increase during mid-exponential phase to compensate for the decline of transcription from the *rrnB* promoter during this period.

3.3. Fluorescence of the *p*rrnB::gfp *reporter strain during balanced growth*

Strains Rm1021/pKW1 and Rm1021/pTSM2 were grown in batch culture in five media that supported different growth rates. These were M9-glycerol, M9-succinate, M9-fumarate, TY, and TY+glucose. To ensure that the cultures grew at a characteristic rate for an extended period and did not reach the density at which the p*rrnB-gfp* reporter was downregulated they were always diluted be-
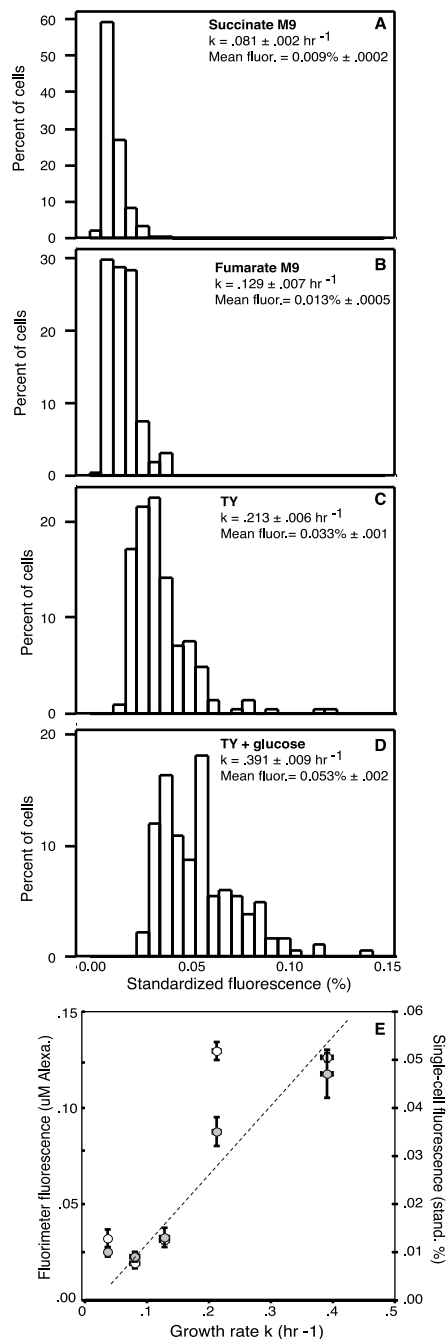
Fig. 3. Fluorescence of strain Rm1021/pKW1 during steady-state growth in media that support different growth rates. A–D: Histograms of single-cell fluorescence values of Rm1021/pKW1 grown in four different media. E: Single-cell (open circles) and fluorimeter (gray circles) determination of Rm1021/pKW1 fluorescence as a function of growth rate. All panels show values from three parallel cultures for each type of growth medium. Error bars in E represent S.E.M. of fluorescence and growth rate. Error bars were often smaller than the circles in the plot.

fore the OD_{415} reached 0.1. After two dilutions, a series of culture samples was taken and the average cellular fluorescence was determined by fluorimetry and microscopic analysis of single cells.

Microscopic analysis showed that, as expected, cells of Rm1021/pKW1 were brighter and larger when growing

quickly than when growing slowly [12,16]. Statistical analysis of single-cell fluorescence showed that the fluorescence distributions were skewed to the left, with right-hand tails that were most pronounced with the faster growing cultures (Fig. 3A–D). The fluorescence distributions of cells growing at different rates overlapped. In spite of this, the means of the fluorescence distributions were quite different for cells grown in four of the five media and the differences between these means were statistically significant (Fig. 3A–E). Fluorescence measurement by fluorimetry also showed that cellular fluorescence increased with increasing growth rates (Fig. 3E).

The *rrnB::gfp* fusion described in this paper has allowed us to begin studies on the transcriptional control of rRNA synthesis in *S. meliloti*. Control of ribosome synthesis is undoubtedly important to the overall cellular economy of this species as in other bacteria.

Recent work by Wells and Long suggests that control of ribosome synthesis may be intimately integrated with nodulation in *S. meliloti* [31]. They have shown that guanosine tetraphosphate (ppGpp), an alarmone that downregulates ribosome synthesis in a variety of bacteria [31–35], is synthesized in *S. meliloti* by a protein that has domains similar to RelA and SpoT. These are proteins that synthesize and degrade ppGpp in *E. coli* [14,36,37]. A *S. meliloti* mutant strain deficient for this *relA/spoT* gene failed to synthesize ppGpp, overproduced succinoglycan and was deficient in nodule formation [31], indicating there may be a connection between control of ribosome synthesis and the establishment of symbiosis.

Acknowledgements

References

[1] Brewin, N.J. (1991) Development of the legume root nodule. Annu. Rev. Cell Biol. 7, 191–226.

[2] Denarie, J., Debelle, F. and Prome, J.C. (1996) *Rhizobium* lipo-chitooligosaccharide nodulation factors: Signaling molecules mediating recognition and morphogenesis. Annu. Rev. Biochem. 65, 503–535.

[3] Hirsch, A.M. (1999) Role of lectins (and rhizobial exopolysaccharides) in legume nodulation. Curr. Opin. Plant Biol. 2, 320–326.

[4] Long, S.R. (1996) *Rhizobium* symbiosis: nod factors in perspective. Plant Cell 8, 1885–1898.

[5] Mylona, P., Pawlowski, K. and Bisseling, T. (1995) Symbiotic nitrogen fixation. Plant Cell 7, 869–885.

[6] Spaink, H.P. (1995) The molecular basis of infection and nodulation by rhizobia: The ins and outs of sympathogenesis. Annu. Rev. Phytopathol. 33, 345–368.

[7] Finan, T.M. et al. (2001) The complete sequence of the 1,683-kb pSymB megaplasmid from the N_2-fixing endosymbiont *Sinorhizobium meliloti*. Proc. Natl. Acad. Sci. USA 98, 9889–9894.

[8] Galibert, F. et al. (2001) The composite genome of the legume symbiont *Sinorhizobium meliloti*. Science 293, 668–672.

[9] Stowers, M.D. (1985) Carbon metabolism in *Rhizobium* species. Annu. Rev. Microbiol. 38, 89–108.

[10] Graham, P.H. (1964) Studies on the utilisation of carbohydrates and Krebs cycle intermediates by Rhizobia, using an agar plate method. Antonie van Leeuwenhok 30, 68–72.

[11] Miura, A., Krueger, J.H., Itoh, S., de Boer, H.A. and Nomura, M. (1981) Growth-rate-dependent regulation of ribosome synthesis in *E. coli* expression of the *lacZ* and *galK* genes fused to ribosomal promoters. Cell 25, 773–782.

[12] Schaechter, M., Maaloe, O. and Kjeldgaard, N.O. (1958) Dependency on medium and temperature of cell size and chemical composition during balanced growth of *Salmonella typhimurium*. J. Gen. Microbiol. 19, 592–606.

[13] Young, R. and Bremer, H. (1976) Polypeptide-chain-elongation rate in *Escherichia coli* B/r as a function of growth rate. Biochem. J. 160, 185–194.

[14] Gourse, R.L., Gaal, T., Bartlett, M.S., Appleman, J.A. and Ross, W. (1996) rRNA transcription and growth rate-dependent regulation of ribosome synthesis in *Escherichia coli*. Annu. Rev. Microbiol. 50, 645–677.

[15] Bremer, H. and Dennis, P.P. (1987) in: *Escherichia coli* and *Salmonella typhimurium*: Cellular and Molecular Biology, Vol. 2 (Umbarger, H.E., Ed.), pp. 1527–1542. American Society for Microbiology, Washington, DC.

[16] Ramos, C., Molbak, L. and Molin, S. (2000) Bacterial activity in the rhizosphere analyzed at the single-cell level by monitoring ribosome contents and synthesis rates. Appl. Environ. Microbiol. 66, 801–809.

[17] Aiyar, S.E., Gaal, T. and Gourse, R.L. (2002) rRNA promoter activity in the fast-growing bacterium *Vibrio natriegens*. J. Bacteriol. 184, 1349–1358.

[18] Gustafson, A.M., O'Connell, K.P. and Thomashow, M.F. (2002) Regulation of *Sinorhizobium meliloti* 1021 *rrnA*-reporter gene fusions in response to cold shock. Can. J. Microbiol. 48, 821–830.

[19] Hirvonen, C.A., Ross, W., Wozniak, C.E., Marasco, E., Anthony, J.R., Aiyar, S.E., Newburn, V.H. and Gourse, R.L. (2001) Contributions of UP elements and the transcription factor FIS to expression from the seven *rrn* P1 promoters in *Escherichia coli*. J. Bacteriol. 183, 6305–6314.

[20] Sambrook, J., Fritsch, E.F. and Maniatis, T. (1989) Molecular Cloning: A Laboratory Manual, 3rd edn. Cold Spring Harbor Laboratory Press, Cold Spring Harbor, NY.

[21] Cormack, B.P., Valdivia, R.H. and Falkow, S. (1996) FACS-optimized mutants of the green fluorescent protein (GFP). Gene 173, 33–38.

[22] Oke, V. and Long, S.R. (1999) Bacterial genes induced with the nodule during the *Rhizobium*-legume symbiosis. Mol. Microbiol. 32, 837.

[23] Gage, D.J., Bobo, T. and Long, S.R. (1996) Use of green fluorescent protein to visualize the early events of symbiosis between *Rhizobium meliloti* and alfalfa, *Medicago sativa*. J. Bacteriol. 178, 7159–7164.

[24] Daniels, L., Hanson, R.S. and Phillips, J.A. (1994) in: Methods for General and Molecular Biology (Kreig, N.R., Ed.), pp. 512–554. American Society for Microbiology, Washington, DC.

[25] Galibert, F., Batut, J., Goffeau, A., Portetelle, D., Pohl, T., Puhler, A., Finan, T.M. and Long, S.R., http://sequence.toulouse.inra.fr/rhime/Complete/doc/Complete.html.

[26] Capela, D. et al. (2001) Analysis of the chromosome sequence of the legume symbiont *Sinorhizobium meliloti* strain 1021. Proc. Natl. Acad. Sci. USA 98, 9877–9882.

[27] Condon, C., Squires, C. and Squires, C.L. (1995) Control of rRNA transcription in *Escherichia coli*. Microbiol. Rev. 59, 623–645.

[28] Cheng, H.-P. and Walker, G.C. (1998) Succinoglycan is required for

initiation and elongation of infection threads during nodulation of alfalfa by *Rhizobium meliloti*. J. Bacteriol. 180, 5183–5191.

[29] Andersen, J.S., Sternberg, C., Poulsen, L.K., Bjørn, S.P., Givskov, M. and Molin, S. (1998) New unstable variants of green fluorescent protein for studies of transient gene expression in bacteria. Appl. Environ. Microbiol. 64, 2240–2246.

[30] Egelhoff, T.T. and Long, S.R. (1985) *Rhizobium meliloti* nodulation genes: Identification of *nodDABC* gene products, purification of *nodA* protein, and expression of *nodA* in *Rhizobium meliloti*. J. Bacteriol. 164, 591–599.

[31] Wells, D.H. and Long, S.R. (2002) The *Sinorhizobium meliloti* stringent response affects multiple aspects of symbiosis. Mol. Microbiol. 43, 1115–1127.

[32] Bugrysheva, J., Dobrikova, E.Y., Godfrey, H.P., Sartakova, M.L. and Cabello, F.C. (2002) Modulation of *Borrelia burgdorferi* stringent response and gene expression during extracellular growth with tick cells. Infect. Immun. 70, 3061–3067.

[33] Eymann, C., Homuth, G., Scharf, C. and Hecker, M. (2002) *Bacillus subtilis* functional genomics: global characterization of the stringent response by proteome and transcriptome analysis. J. Bacteriol. 184, 2500–2520.

[34] Singer, M. and Kaiser, D. (1995) Ectopic production of guanosine penta- and tetraphosphate can initiate early developmental gene expression in *Myxococcus xanthus*. Genes Dev. 9, 1633–1644.

[35] Zusman, T., Gal-Mor, O. and Segal, G. (2002) Characterization of a *Legionella pneumophila relA* insertion mutant and roles of RelA and RpoS in virulence gene expression. J. Bacteriol. 184, 67–75.

[36] Hernandez, V.J. and Bremer, H. (1991) *Escherichia coli* ppGpp synthetase II activity requires *spoT*. J. Biol. Chem. 266, 5991–5999.

[37] Pedersen, F.S., Lund, E. and Kjeldgaard, N.O. (1977) Analysis of the *relA* gene product of *Escherichia coli*. Eur. J. Biochem. 76, 91–97.

[38] Meade, H.M., Long, S.R., Ruvkun, G.B., Brown, S.E. and Ausubel, F.M. (1982) Physical and genetic characterization of symbiotic and auxotrophic mutants of *Rhizobium meliloti* induced by transposon Tn5 mutagenesis. J. Bacteriol. 149, 114–122.

[39] Bringhurst, R.M., Cardon, Z.G. and Gage, D.J. (2001) Galactosides in the rhizosphere: utilization by *Sinorhizobium meliloti* and development of a biosensor. Proc. Natl. Acad. Sci. USA 98, 4540–4545.

[40] Barnett, M.J., Oke, V. and Long, S.R. (2000) New genetic tools for use in the Rhizobiaceae and other bacteria. Biotechniques 29, 240–245.